Dimensional enhancements in a quantum battery with imperfections

Srijon Ghosh and Aditi Sen(De) ⬤

Harish-Chandra Research Institute, A CI of Homi Bhabha National Institute, Chhatnag Road, Jhunsi, Prayagraj - 211019, India

We show that the average power output of a quantum battery based on a quantum interacting spin model, charged via a local magnetic field, can be enhanced with the increase of spin quantum number, thereby exhibiting dimensional advantage in quantum batteries. In particular, we demonstrate such increment in the power output when the initial state of the battery is prepared as the ground or canonical equilibrium state of the spin-j XY model and the bilinear-biquadratic spin-j Heisenberg chain (BBH) in presence of the transverse magnetic field and a weak value of interaction strength between the spins in the former model. Interestingly, we observe that in the case of the XY model, a tradeoff relation exists between the range of interactions in which the power increases and the dimension, while for the BBH model, the improvements depend on the phase in which the initial state is prepared. Moreover, we exhibit that such dimensional advantages persist even when the battery Hamiltonian has some defects or when the initial battery state is prepared at finite temperature.

I. INTRODUCTION

Quantum computational and communication devices are typically designed using two-level systems. It is also believed that a spin system with a large spin quantum number representing a higher dimensional system loses its quantum nature, thereby showing a classical feature. In contrast, it was shown that the singlet state of arbitrary spin j can violate the Bell inequality maximally even when j is arbitrarily large [1,2]. Over the last two decades, it was also demonstrated that higher dimensional quantum systems, qudits, can deliver advantages over two-level systems in quantum protocols ranging from quantum computation, to topological codes, to quantum purification, to quantum communication including quantum key distribution having an improved key rate [3–13] (see the review on quantum technologies with qudits [14]). For example, it was recently shown that the performance of a quantum switch, a device in which depending on the control qubit operations are performed on the target qubit, can be enhanced by using qudits [15]. Moreover, higher dimensional systems using physical substrates like photons [16], ion traps [17], superconducting circuits [18], and nitrogen-vacancy centers [19] are prepared in laboratories to exhibit quantum information processing tasks.

From a different perspective, quantum spin models with higher spin values have also attracted lots of attention. One of the main reasons for such extensive investigations is that the characteristics of the half-integer spin system can be completely different than that of the integer-spin models. Specifically, Haldane's conjecture states that antiferromagnetic spin chains having half-integer and integer spins possess contrasting properties in terms of excitation spectra [20–27]. Moreover, nonmagnetic phases like Haldane, dimerized, and nematic phases are reported in spin models with arbitrary large spins compared to a spin-$\frac{1}{2}$ chain.

All these results indicate that the quantum devices based on the quantum spin-j model may lead to a better efficiency than that of the quantum spin-$\frac{1}{2}$ model. In this paper, we will demonstrate that it is indeed the case by considering an energy storage device, a quantum battery [28–47]. A ground state or canonical equilibrium state of an interacting Hamiltonian is the initial state of the battery [34,39] while the energy is stored (extracted) in (from) the battery by applying a local magnetic field. In recent years, a considerable amount of works have been carried out to understand the performance of the quantum battery in presence of decoherence, impurities, etc., and the property of the system which leads to quantum advantage. However, all the investigations are restricted to multiqubit systems except for very few recent works on three-level systems [37,38].

In this paper, we consider a one-dimensional anisotropic transverse XY quantum spin model [24,48,49] and bilinear-biquadratic Heisenberg (BBH) spin chain with arbitrary large spins [50–57] as a quantum battery. In particular, the system consists of N spin-j particles and its ground state is taken as the initial state which evolves via a local charging field by unitary evolution. We calculate the maximum extractable power from the battery by varying j and find in both the models that power output is enhanced with the increase of spin quantum number. However, the beneficiary character of quantum batteries in higher dimensions is not ubiquitous. Specifically, we show both analytically and numerically that the improvement with high j in terms of power can only be observed when the interaction strength is weak for the quantum XY model and with low anisotropy. On the other hand, for the bilinear-biquadratic Heisenberg model, we again report the dimensional advantage although the enhancement depends on the phase of the initial state.

From an experimental point of view, such a scenario described above is ideal. We now introduce imperfections in

two ways: (1) the finite-temperature state is considered as the initial state and and (2) impurity is present in the battery Hamiltonian which naturally arises during the preparation of the system. Surprisingly, we observe that for the XX model, although the energy stored (extracted) in (from) the battery increases with the increase of dimension for the low-temperature regime, when the temperature in the thermal state is high, the opposite picture develops—spin models with low spin quantum number exhibit higher power output compared to that of the higher dimensional battery. In presence of defects in the interaction strength which are site dependent and chosen randomly from Gaussian distribution, we find that dimensional enhancement persists in the quenched average power both for the XX as well as bilinear-biquadratic models in presence of weak disorder strength quantified by the standard deviation of the distribution.

The paper is presented as follows. After describing the prerequisites at the beginning of Sec. II, we analytically show in Sec. II A that a battery built by using a spin-1 XX chain results in more output power than that obtained via a spin-$\frac{1}{2}$ XX chain and then we establish the dimensional advantage for several values of j. The next section (in Sec. III) reveals that the performance of the battery depends both on the dimension and the phase of an isotropic bilinear-biquadratic Hamiltonian. Section IV deals with the scenarios when the initial state is prepared at finite temperature or the battery Hamiltonian has some randomness in the interaction strength. Finally, in Sec. V, we summarize the results.

II. ENHANCED BATTERY POWER WITH THE INCREASE OF SPIN QUANTUM NUMBER: ILLUSTRATION BY TRANSVERSE XY MODEL

A quantum battery is modeled as a finite number of quantum-mechanical interacting systems in d dimensions, governed by a Hamiltonian, H_B^j, with j being the spin quantum number, indicating the dimension of the battery. To charge the system, a local magnetic field, governed by the Hamiltonian, H_c^j, is applied to each subsystem. The initial state, $\rho(0)$, of the battery, is taken to be the ground state or the canonical equilibrium state of the Hamiltonian H_B^j.

Our main motivation is to figure out the effects of higher dimensions on the energy storage and extraction processes of the quantum battery. In a closed system, the total work output from the battery is defined as [28,29] $W(t) = W_{\text{final}} - W_{\text{initial}} = \text{Tr}[H_B^j \rho(t)] - \text{Tr}[H_B^j \rho(0)]$, where the initial energy of the system is $\text{Tr}[H_B^j \rho(0)]$ and $\rho(t)$ represents the dynamical state of the battery at time t which is obtained when the local charger $U(t)$ acts on the initial state $\rho(0)$, i.e., $\rho(t) = U(t)\rho(0)U(t)^\dagger$ with $U(t) = e^{-iH_c^j t}$. Notice that the storing energy in the battery may not always be the same with the maximum energy that can be extracted from the battery, quantified via ergotropy [28] (see [35,47]). However, we will show that in our system, both the quantities coincide when the ground state of the battery acts as the initial state. The maximum average power output from the system, in our case, reads as $P_{\text{max}} = \max_t \frac{W(t)}{t}$.

Our main aim is to obtain a comparative study in the efficiency of the battery in terms of P_{max} with increasing the

dimension of the system. To put all the models in arbitrary dimension on the same footing, we confine the spectrum of the battery Hamiltonian in $[-1, 1]$ by normalizing it [39] as $\frac{[2H_B - (e_{\text{max}} + e_{\text{min}})\mathbb{1}]}{e_{\text{max}} - e_{\text{min}}}$, where e_{max} and e_{min} are the maximum and minimum eigenvalues of the original Hamiltonian, respectively. We now argue that if the battery is initially prepared as the ground (thermal) state of the spin-j Hamiltonian, we can increase the power of the battery with the increase of the dimension j when the charging is performed by the local field.

A. Transverse spin-j XY model as a quantum battery and its charging process

Before presenting the results, let us first describe the one-dimensional anisotropic quantum XY spin chain consisting of N spin-j particles [22,24,27,48,49,58] the ground (thermal) state of which acts as an initial state of the battery. In this paper, we consider the model having the nearest-neighbor interactions among the spins and with open boundary condition. The spin-j XY battery Hamiltonian, H_B^j, reads as

$$
H_B^j = \frac{1}{2}h\sum_{k=1}^{N} S_k^z
$$
$$
+ \frac{1}{4}\sum_{k=1}^{N-1} J_k\big[(1+\gamma)S_k^x \otimes S_{k+1}^x + (1-\gamma)S_k^y \otimes S_{k+1}^y\big],
$$
$$
(1)
$$

where S_k^i are the spin matrices with $i = x, y, z$ acting on site k. E.g., for spin-1/2 particles, i.e., when $j = 1/2$, S_k^i represents the spin Pauli matrices. Here J_k is the site-dependent interaction strength between the particles, h is the external magnetic field, and γ is the anisotropy parameter. Notice that $\gamma = 0$ and 1 correspond to the spin-j XX and Ising models, respectively. When $J_k = J$, i.e., we remove the site dependence in the coupling, the model reduces to the ordered system, otherwise it is disordered. As mentioned before, we normalize the spectrum of the Hamiltonian between -1 and 1. The magnetic field applied to charge the battery at each site is given by

$$
H_c^j = \frac{\omega}{2}\sum_{k=1}^{N} S_k^x,
$$
$$
(2)
$$

where ω is the strength of the magnetic field.

Increment in power with the variation of dimensionality: Spin-$\frac{1}{2}$ vs spin-1 chain

Let us prepare the initial state of the battery as the ground state (i.e., the zero-temperature state) of H_B^j with $j = 1/2$ or 1 consisting of two spins. The corresponding H_c^j is applied to store the energy in the battery. We will now show that when interaction strength between the two sites is weak, i.e., when $J_k/|h| = J/|h| = \lambda$ is small, maximum achievable power (P_{max}) increases with the increase of the dimension of the spins. Later we will provide evidence that the results hold even for a spin chain with four sites containing a higher number of spins.

Proposition 1. If the initial state of the battery is the ground state, i.e., the zero-temperature state of the spin-1 transverse
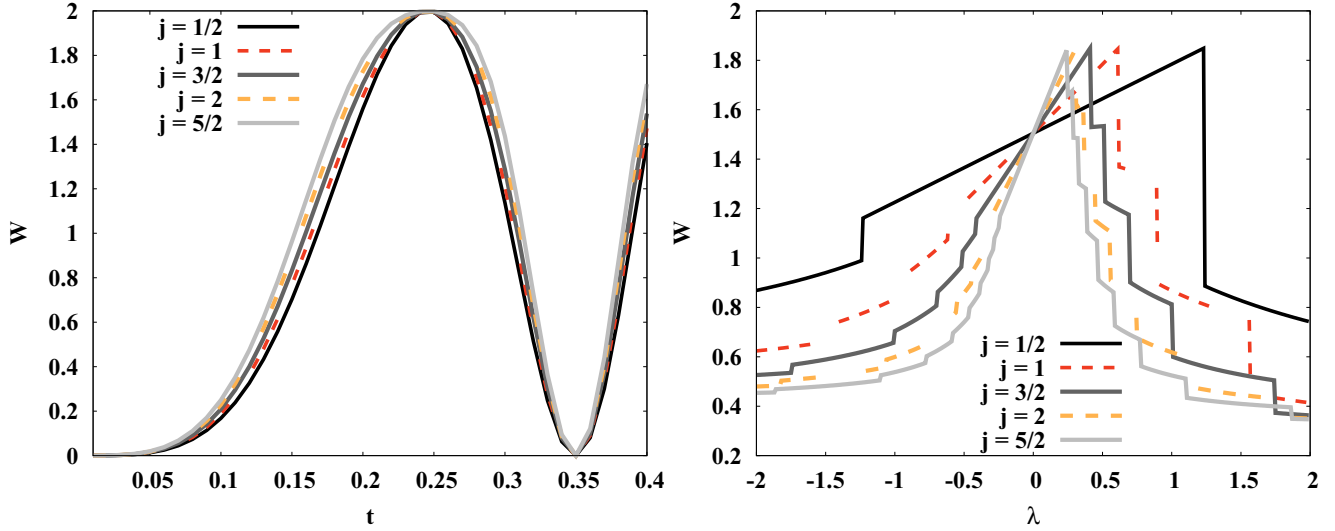
FIG. 1. Amount of stored work $W(t)$ (ordinate) against time t (abscissa) (left panel) and with λ (abscissa) (right panel) for the transverse XX model, i.e., for $\gamma = 0$ with different values of spin quantum number, j. Solid and dashed lines represent half-integer and integer spins, respectively. Dark, gray, and light gray indicate the increment in the dimension in both the cases. For illustration, we fix $\lambda = 0.2$ for the left panel while $t = 2.1$ for the right panel. Here $N = 4$. We also notice that in this model, the extractable work from the battery, the ergotropy [28], coincides with the work output (see [35,47]). All the axes are dimensionless.

XX model, the maximum average power of the battery, $P_{\max}$, is higher than that of the XX model consisting of spin-1/2 particles provided the interaction strength between the sites is weak.

Proof. Let us first calculate the maximum average power of the battery consisting of two spin-$\frac{1}{2}$ particles with $\gamma = 0$. Without loss of generality, we consider the strength of the charging field (ω) to be unity. The Hamiltonian in this case takes the form

$$H_B^{j=1/2} = \begin{pmatrix} 1 & 0 & 0 & 0 \\ 0 & 0 & \lambda/2 & 0 \\ 0 & \lambda/2 & 0 & 0 \\ 0 & 0 & 0 & -1 \end{pmatrix}, \quad (3)$$

which has the normalized ground state $\rho^{j=1/2}(0) = |11\rangle\langle 11|$ as the initial state. The corresponding initial energy is $W_{\text{initial}} = -1$. After the evolution according to $H_c^{j=1/2}$, the evolved state at time t looks like

$$\rho^{j=1/2}(t) = \begin{pmatrix} \frac{B^2}{4} & \frac{-iB\sin t}{4} & \frac{-iB\sin t}{4} & -\frac{AB}{4} \\ \frac{-B\sin t}{4i} & \frac{\sin^2 t}{4} & \frac{\sin^2 t}{4} & \frac{A\sin t}{4i} \\ \frac{-B\sin t}{4i} & \frac{\sin^2 t}{4} & \frac{\sin^2 t}{4} & \frac{A\sin t}{4i} \\ -\frac{AB}{4} & \frac{iA\sin t}{4} & \frac{iA\sin t}{4} & \frac{A^2}{4} \end{pmatrix}, \quad (4)$$

where $(1 + \cos t) = A$ and $(1 - \cos t) = B$ and the final energy reads as

$$W_{\text{final}} = (a\cos t + b\lambda \sin^2 t), \quad (5)$$

where $a = -0.999\,698 \approx -1$ (which is actually equal with W_{initial} at $t = 0$) and $b = 0.25$ with $\omega = 1$ (see Fig. 1 with $N = 4$). Note that a and b depend on ω. For any values of λ, we can maximize the work with respect to time, thereby obtaining the power. E.g., for $\lambda = 0.2$, we find that $P_{\max}^{j=\frac{1}{2}} = \max_t \frac{W_{\text{final}} - W_{\text{initial}}}{t} = 0.7370$, which occurs at time $t = 2.23$. We

will restrict only to the situation when λ is small and positive. Note that the choice of λ up to which the battery Hamiltonian performs better than the classical one depends on j (see Table I). [Notice that when the battery Hamiltonian in Eq. (1) is without the interaction term, i.e., $J_k = 0$, we refer the model as the classical model of the battery.]

Following the same prescription, we now evaluate $P_{\max}^{j=1}$ for the spin-1 XX model. In the computational basis, the Hamiltonian reads as

$$\begin{aligned} H_B^{j=1} &= (|00\rangle\langle 00| - |22\rangle\langle 22|) + \frac{1}{2}(|01\rangle\langle 01| + |10\rangle\langle 10|) \\ &\quad + \frac{1}{2}(|12\rangle\langle 12| - |21\rangle\langle 21|) \\ &\quad + \frac{\lambda}{2}(|01\rangle\langle 10| + |02\rangle\langle 11| + |10\rangle\langle 20| + |11\rangle\langle 21|) \\ &\quad + \text{H.c.}, \end{aligned} \quad (6)$$

and the initial state $\rho^{j=1}(0)$ becomes $|22\rangle\langle 22|$. After evolving the state, the final state at time t reads as $|\psi^{j=1}(t)\rangle = a(t)(|00\rangle + |22\rangle) + b(t)|01\rangle + c(t)(|02\rangle + |10\rangle + |20\rangle + |21\rangle) + d(t)|11\rangle + e(t)|12\rangle$. Here $a(t) = 0.37 + 0.06e^{-2it} + 0.06e^{2it} - 0.5\cos t$, $b(t) = i(0.35\sin t - 0.16\sin 2t)$, $c(t) = -0.125 + 0.06e^{-2it} + 0.06e^{2it}$, $d(t) = -0.25 + 0.13e^{-2it} + 0.13e^{2it}$, and $e(t) = i(-0.35\sin t - 0.16\sin 2t)$.

In this case, $W_{\text{initial}} = -1$ and $W_{\text{final}} = -\cos t + 0.25\lambda(1 - \cos t)$, we calculate the power at time t, which can be represented as

$$\begin{aligned} P^{j=1}(t) &= a' - b'\cos t + \cos t(-b' - c'\cos t) \\ &\quad + [-2(1 - a') - c'\cos t + (1 - a')\cos 2t]\cos 2t \\ &\quad + 0.05\sin^2 t - \frac{\sin t \sin^2 t}{4} + (1 - a')\sin^2 t, \quad (7) \end{aligned}$$
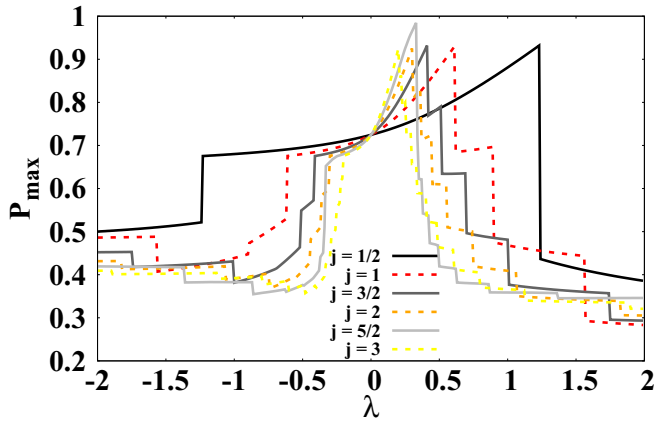
FIG. 2. $P_{\max}$ vs λ for the transverse XX model. Solid lines indicate half-integer spins while the dashed ones depict integer spins. Moreover, the dimension of the system increases from dark to light shade in each scenario. In the legend, j indicates the spin quantum number of each site. Here $N = 4$. Clearly, there is a region in λ where higher dimensional systems perform better than low dimensional models. Both the axes are dimensionless.
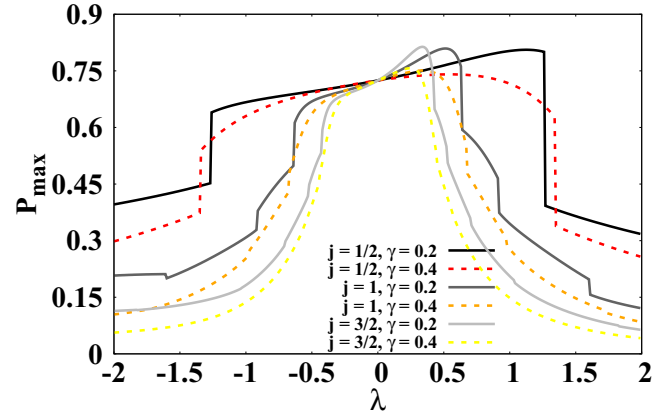

FIG. 3. $P_{\max}$ against λ of the transverse XY model for different values of j and anisotropy parameters γ. Solid lines and dashed lines are for $\gamma = 0.2$ and 0.4, respectively. The value of dimension increases from dark to light gray shades in both the cases. This shows that along with λ, anisotropy parameters also play a crucial role to obtain dimensional advantage. Other specifications are the same as Fig. 2. Both the axes are dimensionless.

where a', b', and c' are functions of λ as well as ω. By maximizing over time and considering the same $\lambda = 0.2$ as in the case of spin-$\frac{1}{2}$ systems, we obtain $P_{\max}^{j=1} = 0.752\,296$, which is clearly higher than that obtained for spin-$\frac{1}{2}$ systems, i.e., $P_{\max}^{j=\frac{1}{2}} < P_{\max}^{j=1}$ with $\lambda = 0.2$. By using Eqs. (5) and (7), we can always find that when λ is weak, the storage capacity of the battery increases with j. For example, with $\lambda = 0.1$, $P_{\max}^{j=\frac{1}{2}} = 0.7304 < P_{\max}^{j=1} = 0.7371$ while $\lambda = 0.5$ gives $P_{\max}^{j=\frac{1}{2}} = 0.7608 < P_{\max}^{j=1} = 0.8145$. ∎

Remark 1. Although the hierarchy among power in Proposition 1 is proven by comparing $j = 1/2$ and 1, it can be shown to be true for other higher dimensional systems as well, for small values of λ (see Fig. 2 and Table I). Such a result can be intuitively understood as follows: for a weak or negligible interaction strength, the spins are initially pointing towards the z direction due to the external magnetic field of the battery Hamiltonian at zero temperature for a given dimension. Since the charging field is applied in the x direction, aligning the spins along the direction of the charging field requires more energy for driving the system out of equilibrium than that of the battery Hamiltonian with higher interaction strength which leads to a generation of a higher amount of work in the former case. In addition, the gap between the maximum and the minimum energy increases with the increase of dimension and hence the charging field needs to do more work to drive

the system away from equilibrium in the higher dimensional battery, thereby producing a higher amount of power for a fixed value of λ and γ compared to a low-dimensional battery. As shown in Fig. 1, the work is oscillating with time, although its maximum value is fixed. Since $W(t)$ is a strictly increasing function of time between the initial time and the time when it reaches its maximum value which leads to the power generation, the argument for the stored energy can also be applied for the power output and hence a similar dimensional advantage in the case of power is also observed as depicted in Fig. 3. We will show in the next subsection that the results also hold for a moderate value of interaction strength.

Remark 2. Proposition 1 also holds for the XY-spin models, i.e., for spin models with nonvanishing anisotropy parameter, γ. For a given dimension, there exists a critical anisotropy parameter above which no "quantum advantage" can be seen (see Figs. 3 and 5). Since $\lambda = 0$ in Eq. (1) leads to the battery Hamiltonian, which is local having no interaction term, the ground or the thermal state of the battery cannot have any quantum feature like entanglement and hence $P_{\max}$ which is more than that obtained via $\lambda = 0$ can be termed as quantum advantage.

B. Power of a quantum battery built up via quantum XY model in arbitrary dimensions

By comparing maximum power output of the battery prepared by using quantum spin-$\frac{1}{2}$ and spin-1 chains, we have already got an indication that the storage capacity of the energy in a battery can be enhanced by increasing the dimension of the model. To analyze the effect of dimensions on work extraction of the battery, the initial state of the battery is prepared as the ground state of the anisotropic spin-j XY chain. Let us start by studying the variation of stored energy, $W(t)$, of the battery with respect to time for a fixed value of interaction
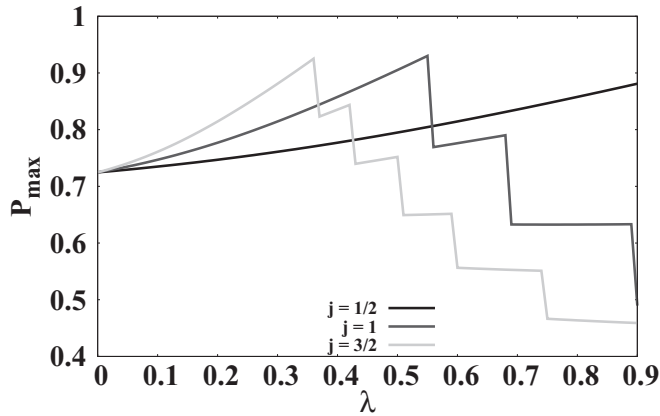
TABLE I. Maximum values of interaction strength, $\lambda_{\max}$, for which $P_{\max}$ reaches its maximum for fixed dimensions of spins, j. We choose two anisotropy parameters of the XY model for analysis, specifically, $\gamma = 0$ and 0.2.

j	$\frac{1}{2}$	1	$\frac{3}{2}$	2	$\frac{5}{2}$	3
$\lambda_{\max}(\gamma = 0)$	1.23	0.61	0.41	0.30	0.33	0.20
$\lambda_{\max}(\gamma = 0.2)$	1.15	0.51	0.33	0.25	0.26	0.17

FIG. 4. $P_{\max}$ against λ of the transverse XY model for different values of j and $\gamma = 0$. Here $N = 6$. Both the axes are dimensionless.
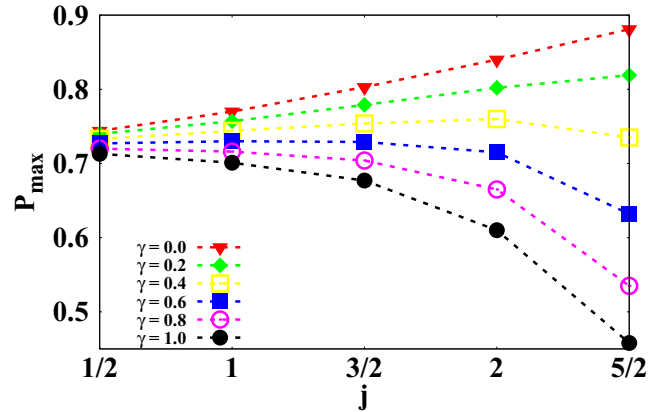

FIG. 5. Variation of $P_{\max}$ (ordinate) of the XY battery Hamiltonian with respect to spin quantum numbers, j (abscissa). Different symbols correspond to different strengths of the anisotropy, γ. The interaction strength is fixed to $\lambda = 0.2$. Both the axes are dimensionless.

strength, and the behavior of work output against the interaction strength λ for a fixed value of time (see Fig. 1). Here one must note that there is no optimization over time. Moreover, we notice that $W(t)$ coincides with the maximum extractable work from the battery, i.e., ergotropy [28]. We observe that both in the oscillatory dynamics of extracted work and in the variation of work with respect to λ, the dimensional advantage persists; i.e., by increasing the value of spin quantum number j, it is possible to store more energy in the battery. To make the analysis more concrete, we compute the maximum power output from the battery, and in the rest of the paper, we discuss the performance of the quantum battery in terms of $P_{\max}$.

The entire analysis is performed by considering a spin chain consisting of four sites. We cannot go beyond that number since the size of the matrices involved in the computation increases with j, thereby restricting the numerical simulation of the dynamics. Note, however, that the performance remains qualitatively similar even if we consider the battery Hamiltonian with a large number of spins which we check for small dimensions (see Fig. 4 for $N = 6$). The observations regarding the interplay between the dimension, the interaction strength, and the anisotropy are listed below.

1. Tradeoff between dimension and interaction strength

Let us first carry out the analysis of a quantum battery by fixing $\gamma = 0.0$. As depicted in Fig. 2, with the increase of dimension of the spins, the maximum average power ($P_{\max}$) of the system increases monotonically when $0 < \lambda \leqslant \lambda_{\max}$, where $\lambda_{\max}$ denotes the maximum value of the interaction strength for which $P_{\max}$ reaches its maximum value. Interestingly, notice that after an increase for low j, $P_{\max}$ saturates along with the range of λ, giving an advantage, for high values of j. In particular, from the figure, we observe that the slope of $P_{\max}$ remains almost the same with the further increase of j. Hence we can possibly conjecture that in arbitrary dimension the power output gives a nonclassical enhancement in power in presence of weak interactions. As found in Table I, $\lambda_{\max}$ decreases with j. This implies that the advantage obtained in

a higher dimensional spin chain comes at the cost of more control on the interaction strength.

2. Role of anisotropy in power

Along with the coupling constant, the anisotropy between the interaction strength in the xy plane also plays a crucial role in power extraction. In particular, increase of anisotropy decreases the enhancement. In other words, the work output in the battery is more pronounced for the XX model compared to the XY model with $\gamma \neq 0$ as shown in Fig. 3. Since the charging field is in the x direction, for a nonzero value of γ and for a fixed dimension, it will be easier for the charging Hamiltonian to drive the system out of equilibrium, resulting in a lower amount of power generation. To show this more precisely, we define a quantity $\gamma_{\mathrm{critical}}^{\lambda}$. For a fixed value of λ and j, it is defined as the value of the anisotropy parameter up to which we can get dimensional advantage in terms of power extraction from the quantum battery. Up to the numerical accuracy of four decimal places, we report that $\gamma_{\mathrm{critical}}^{0.01} = 0.98$ while $\gamma_{\mathrm{critical}}^{0.1} = 0.8$ for all values of $j \leqslant 3/2$. Moreover, we fix the interaction strength, say, $\lambda = 0.2$, and see the behavior of $P_{\max}$ with j for a different anisotropy. Figure 5 imitates the aforementioned points in a much clarified way with respect to the dimension of the spins. It is clear from this analysis that, with the decrease of λ, the range of γ, i.e., $\gamma_{\mathrm{critical}}^{\lambda}$, increases for a given value of j.

III. PHASE DEPENDENCE OF POWER OUTPUT IN A SPIN-J BILINEAR-BIQUADRATIC CHAIN

Up to now, dimensional improvements in the performance of the battery are illustrated by considering the quantum XY model. A natural question is to find out whether the enhancement persists even for other one-dimensional battery Hamiltonians. To address this question, the ground state of

the spin-j bilinear-biquadratic Hamiltonian is considered as the initial state of the battery [50–56], given by

$$H_B^j(\phi) = \sum_{k=1}^{N-1} J_k [\cos\phi(\overrightarrow{S}_k \cdot \overrightarrow{S}_{k+1})$$
$$+ \sin\phi(\overrightarrow{S}_k \cdot \overrightarrow{S}_{k+1})^2] + \frac{h}{2} \sum_{k=1}^{N} S_k^z. \quad (8)$$

Here, $J_k \cos\phi$ and $J_k \sin\phi$ are the site-dependent interaction strengths, $\overrightarrow{S}_k$ is the spin vector acting on the kth site, and ϕ is the parameter depending on which a rich phase diagram emerges. Without the magnetic field, i.e., when $h = 0$, and for the spin-1 chain, the Haldane phase appears when $-\pi/4 < \phi < \pi/4$ while the gapless critical phase was found when $\pi/4 \leqslant \phi \leqslant \pi/2$ and the system shows ferromagnetism with $-3\pi/4 < \phi < \pi/2$. These three phases and their corresponding phase boundaries are well established although there is a controversy about the critical points of the dimerized phase which is sandwiched between the ferromagnetic and Haldane phases.

To charge the system, we consider quadratic charging field H_c^j of the form

$$H_c^j = \omega \sum_{k=1}^{N} \frac{S_k^x}{2} + \frac{(S_k^x)^2}{4}, \quad (9)$$

where ω is the strength of the charging field.

To demonstrate the influence of ϕ on the energy storage capacity of a quantum battery when the local magnetic field, given in Eq. (9), is applied to charge the battery, we choose three values of ϕ—one is from the Haldane phase, e.g., $\phi = \frac{\pi}{6}$, and the other two are chosen, respectively, from the critical phase, e.g., $\phi = \frac{\pi}{3}$, and from the ferromagnetic phase, say $\phi = \frac{2\pi}{3}$. Unlike the XY model, in all the phases, we notice striking changes in $P_{\max}$ with respect to the interaction strength and with higher dimension. The investigations are carried out with the choices of $j = 1, \frac{3}{2}$, and 2 to show that the power has a significant dependence on phase ϕ.

Phase-dependent dimensional advantage

When $\lambda > 0$, the interaction does not give any quantum advantage for a low dimensional system (see $P_{\max}$ of the battery with $j = 2$), which is in stark contrast with the battery based on the XY spin model. However, the regime, in the parameter space where $\lambda < 0$, develops some interesting features in the bilinear-biquadratic model and so now onwards all the analyses are performed for $\lambda < 0$. It is evident from Fig. 6 that the dimensional advantage persists irrespective of the value of the phase parameter in the initial state. Nonetheless for $j = 1$, the ferromagnetic phase gives beneficial behavior over Haldane and critical phases in terms of $P_{\max}$. However, for higher dimensional systems ($j = 3/2$ or 2), the Haldane phase slowly takes over the other two although the difference between $P_{\max}$ with $\phi = \pi/6$ and that of a battery with $\phi = \pi/3$ or $2\pi/3$ is very small.

In all these cases, we observe two types of improvements in the performance of the battery—one is due to the increase of spin quantum number and other one is for the increase of the
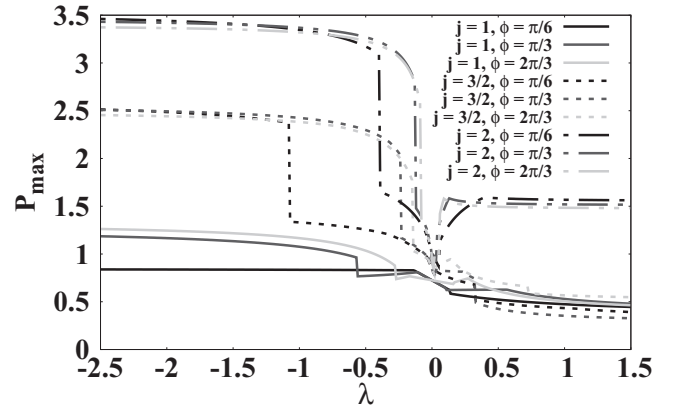

FIG. 6. $P_{\max}$ of the BBH model (vertical axis) against λ (horizontal axis). Solid, dashed, and dot-dashed lines are for the model with $j = 1, 3/2$, and 2, respectively, while black, gray, and light gray represent three different values of $\phi = \pi/6$ (Haldane), $\pi/3$ (critical), and $2\pi/3$ (ferromagnetic), respectively, indicating three different phases of BBH model. Both the axes are dimensionless.

interaction strength in the negative direction (see Fig. 6). Like the XY model, we also notice that the increment obtained for power via spin-1 and spin-$\frac{3}{2}$ chains is much bigger than that of spin-$\frac{3}{2}$ and spin-2 chains. Hence, it can be argued that for a fixed ϕ, $P_{\max}$ saturates to a finite value even in arbitrary large dimension, thereby exhibiting quantum gain in the battery over its classical counterparts.

IV. EFFECTS OF LARGE SPIN PERSISTing EVEN IN PRESENCE OF IMPERFECTIONS

We will now show that the dimensional benefit can also be exhibited when there are imperfections in the battery. In the preceding section, we always prepare the initial state at zero temperature. Let us see the consequence on the power if the initial state of the battery is the canonical equilibrium state with a finite temperature. Moreover, we deal with the scenario when the battery Hamiltonian is disordered, i.e., the interaction strength is site dependent. In both the situations, our aim is to determine whether arbitrary large spin helps in the performance of the battery or not.

A. Temperature-induced power of a quantum battery

We will now probe the situation when the initial state is the canonical equilibrium state, $\rho_{\text{th}} = \frac{e^{-\beta' H_B^j}}{Z}$, where $Z = \text{Tr}(e^{-\beta' H_B^j})$ is the partition function of the system with inverse temperature $\beta' = \frac{1}{k_B T}$ (k_B being the Boltzmann constant and T being the absolute temperature). The charging process follows the same unitary evolution governed by the local Hamiltonian, H_c^j in Eq. (2). For investigations, we set $\beta = |h|\beta'$.

1. Low-temperature region

For large value of β, we notice that higher dimensional spins give a larger amount of power output than that of the low-dimensional systems provided the interaction strength is weak and positive in the XX model as in Fig. 7. It is in a
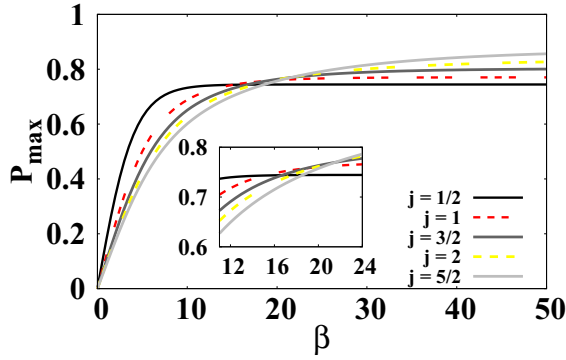
FIG. 7. Dependence of P_{max} (vertical axis) on inverse temperature β (horizontal axis) for different values of j. Here we take $\gamma = 0.0$ and $\lambda = 0.2$. Inset: The region of β where all the lines cross. The rest of the specifications are the same as in Fig. 2. Both the axes are dimensionless.

good agreement with the ground-state case reported before. To make the analysis more concrete, for the XY model, we compute $\beta_{critical}$, the cutoff value of the inverse temperature above which the dimensional enhancement occurs, i.e., where $P_{max}^{j} < P_{max}^{j+\frac{1}{2}}$. From Table II, we observe that $\beta_{critical}$ is increasing with the dimension of the spins, j for the XX model.

On the other hand, for the BBH model, the behavior of P_{max} again turns out to be phase dependent and the tradeoff between phases and dimension still exists as mentioned earlier. We observe that a higher dimensional battery remains beneficial, independent of the choice of ϕ as depicted in Fig. 8.

2. High-temperature region

Interestingly, however, the opposite picture emerges for high values of temperature, i.e., with low β for the XY model having a weak coupling constant of the battery Hamiltonian. Specifically, the spin chain of low dimension is more beneficial than that of the model with large spin. Therefore, we observe a critical temperature $\beta_{critical}$ which separates these two regions (as shown in the inset of Fig. 7). It is prominent that with increasing dimension, $\beta_{critical}$ also increases. As argued before, the higher power generation in the low dimensional system is possibly due to the fact that the charging field in this case requires more energy to drive the system away from equilibrium compared to the higher dimensional systems which can involve a higher number of eigenstates in the process.

Such a critical temperature is not observed in the case of the BBH model; i.e., in the high temperature regime, higher dimensional systems continue to generate a higher amount of

TABLE II. The cutoff value of the inverse temperature, $\beta_{critical}$, of the XY model from which the dimensional advantage is present for a fixed dimensions of spins, j. Here, $\gamma = 0$ and $\lambda = 0.2$.

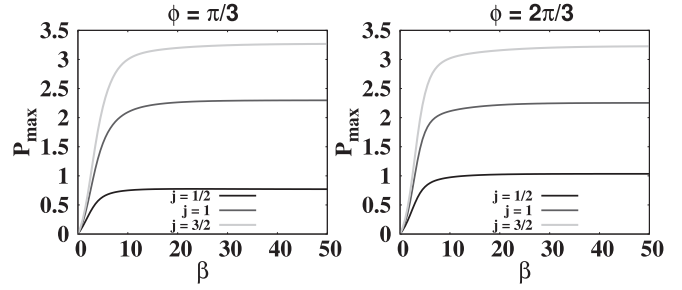| j	1	$\frac{3}{2}$	2	$\frac{5}{2}$
$\beta_{critical}$	15.5	18.5	20	21

FIG. 8. P_{max} (ordinate) with β (horizontal axis) for the BBH model. From below, the dimension increases; i.e., from below, systems with $j = 1$, $3/2$, and 2 are plotted. Left panel: $\phi = \pi/3$. Right panel: $\phi = 2\pi/3$. $\lambda = -0.5$. Both the axes are dimensionless.

power compared to a battery with low dimensions as shown in Fig. 8.

B. Impurity along with large spin leading to an increment in power

We will now concentrate on a battery Hamiltonian which has some defects occurring due to imperfections in the preparation process or due to environmental influence. Here we assume that the change in presence of disorder is very slow compared to the dynamics of the system and hence we can perform "quenched averaging" of the physical quantity.

C. Quench averaging

In both the models considered in the preceding section, we choose randomly the site-dependent interaction strength $J_k/|h|$ from Gaussian distribution with mean $\langle J \rangle / |h| \equiv \langle \lambda \rangle$ and standard deviation, σ_λ. We then compute the maximum power for each choice and repeat the procedure for several times. At the end, we perform averaging over all such realizations, to obtain the quenched averaged power, $\langle P_{max} \rangle$. The number of realizations performed depends on the convergence of the physical quantity. In our paper, we perform 2000 realizations and observe that $\langle P_{max} \rangle$ converges up to second decimal points.

1. Variation of power for the disordered XX model with spin quantum number

The transverse disordered XX spin chain shows dimensional improvements for low values of $\langle \lambda \rangle > 0$ with small disorder strength, σ_λ (see Fig. 9), i.e., $0 < \langle \lambda \rangle < \langle \lambda_{max} \rangle$, $\langle P_{max} \rangle^{j+\frac{1}{2}} > \langle P_{max} \rangle^{j}$. It clearly shows that even if impurity is present in the system, dimensional upgrading in terms of power storage capacity can be obtained.

However, such an advantageous situation vanishes if one increases the strength of the disorder, i.e., the value of σ_λ. It is again due to the tradeoff relation between the interaction strength and the dimensions mentioned in the ordered case. In particular, when interaction strengths are chosen randomly from the Gaussian distribution, we know that, most of the time, interaction strengths lie between $\langle \lambda \rangle \pm 3\sigma_\lambda$ and hence comparing the ordered scenario, we can provide dimensional benefit only for small σ_λ. Precisely, we find that when $\sigma_\lambda > 0.3$, higher values of λ are coming into play, and for the
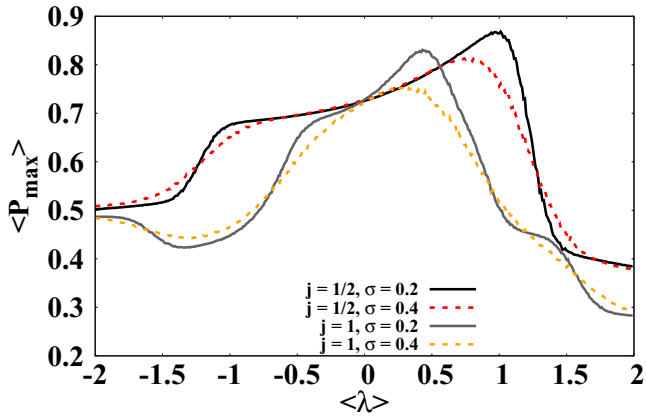
FIG. 9. Quenched averaged power output, $\langle P_{\max} \rangle$ (ordinate) with respect to $\langle \lambda \rangle$ (abscissa) for the disordered XX model. Solid and dashed lines represent $\sigma_\lambda = 0.2$ and 0.4, respectively, while black lines depict spin-$\frac{1}{2}$ systems and light gray lines are for spin-1 particles. Both the axes are dimensionless.

ordered XX model, we found (Table I) that high values of λ do not show any advantage with j. Hence, when strength of the disorder is strong, disordered systems cannot demonstrate any large spin benefit. Moreover, we notice that there exists a small region with $\langle \lambda \rangle < 0$ where the disordered spin-1 XX model gives more power output in comparison with the ordered ones, which is not present in the case of spin-$\frac{1}{2}$ particles.

2. Randomly chosen interaction strength for BBH

As reported before, in the ordered case, when $\lambda < 0$ and $\phi = \frac{2\pi}{3}$, the BBH model with $j = 1$ gives a higher $P_{\max}$ than that of the initial state prepared in a different phase with the same spin quantum number j. A similar situation remains true even in presence of disorder. To illustrate this, we choose $\langle \lambda \rangle < 0$, and $\phi = \frac{\pi}{3}$ and $\frac{2\pi}{3}$. Moreover, we find that with moderately high σ_λ, quenched averaged power $\langle P_{\max} \rangle$ of the

spin-$\frac{3}{2}$ BBH model is significantly higher than that of the spin-1 case, as depicted in Fig. 10.

V. CONCLUSION

In recent times, the ever-increasing demand for energy and limited resources in a classical world is a great threat to humankind. Technologies based on quantum-mechanical principles were shown to overcome the critical situation. In this direction, the classical battery serves a crucial role by converting chemical energy to an electrical one. Nowadays with the emergence of quantum machinery, it is possible to design a *quantum battery* [33,37,38,59,60] which is much smaller in size and way more effective in terms of accumulating accessible energy than the classical ones. From the beginning of its discovery, it is customary to model a quantum battery consisting of spin-$\frac{1}{2}$ particles. Very recently, three-level product states are considered as the initial state of the battery which is charged via an interacting Hamiltonian.

We here constructed a battery the initial state of which is the ground state of an interacting spin-j model and the charging is performed via local unitary operations. We showed the beneficial effects of *dimension* on the performance of the quantum battery. In particular, the ground state, as well as thermal state of the transverse XY spin-chain and BBH Hamiltonian with j-dimensional spins, are used to demonstrate that with the increase of dimensions the power extraction from the system increases. Specifically, we found that in the case of the spin-j XY model the power output depends on the interaction strength as well as the anisotropy parameter while the phase of the initial state plays an important role for the BBH-based battery.

Moreover, in a more realistic situation, we exhibited that the dimensional benefit is robust against the impurities in the battery Hamiltonian or at finite temperature. Notice that both of them naturally appear during implementations. Results obtained here are counterintuitive in the sense that, by increasing the dimensions, it is believed that we typically approach the classical regime although advantages persist even
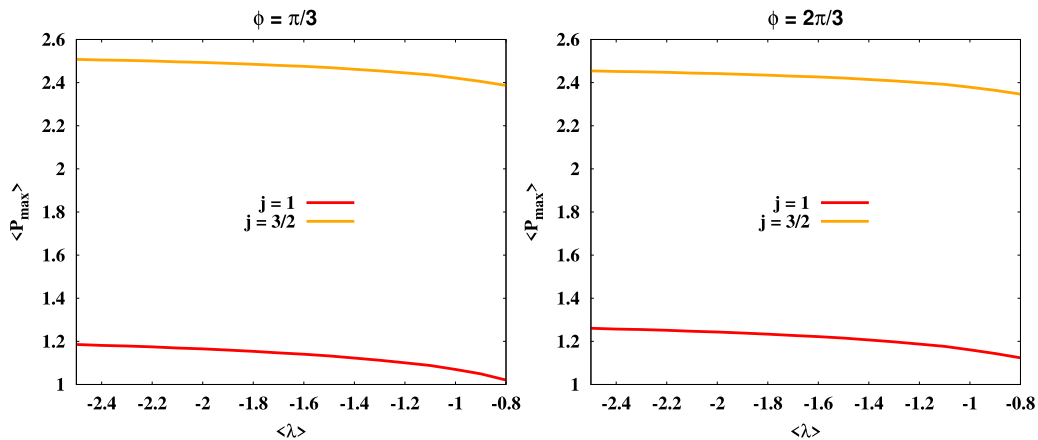

FIG. 10. $\langle P_{\max} \rangle$ (vertical axis) against $\langle \lambda \rangle$ (horizontal axis) for the disordered BBH model. Dark and light lines represent the battery with $j = 1/2$ and 1, respectively. Here we have taken $\sigma_\lambda = 0.2$. Left panel: Critical phase with $\phi = \frac{\pi}{3}$. Right panel: Ferromagnetic phase with $\phi = \frac{2\pi}{3}$. Both the axes are dimensionless.

with arbitrarily large spin which cannot be obtained via the interaction-free battery model.

[1] N. Gisin and A. Peres, Phys. Lett. A **162**, 15 (1992).

[2] A. Garg and N. D. Mermin, Phys. Rev. Lett. **49**, 901 (1982).

[3] S. D. Bartlett, H. de Guise, and B. C. Sanders, Phys. Rev. A **65**, 052316 (2002).

[4] N. J. Cerf, M. Bourennane, A. Karlsson, and N. Gisin, Phys. Rev. Lett. **88**, 127902 (2002).

[5] T. Durt, N. J. Cerf, N. Gisin, and M. Żukowski, Phys. Rev. A **67**, 012311 (2003).

[6] T. Durt, D. Kaszlikowski, J.-L. Chen, and L. C. Kwek, Phys. Rev. A **69**, 032313 (2004).

[7] T. C. Ralph, K. J. Resch, and A. Gilchrist, Phys. Rev. A **75**, 022313 (2007).

[8] T. Vértesi, S. Pironio, and N. Brunner, Phys. Rev. Lett. **104**, 060401 (2010).

[9] F. H. E. Watson, E. T. Campbell, H. Anwar, and D. E. Browne, Phys. Rev. A **92**, 022312 (2015).

[10] P. Skrzypczyk and D. Cavalcanti, Phys. Rev. Lett. **120**, 260401 (2018).

[11] J. Miguel-Ramiro and W. Dür, Phys. Rev. A **98**, 042309 (2018).

[12] A. Fonseca, Phys. Rev. A **100**, 062311 (2019).

[13] S. Roy, S. Mal, and A. Sen(De), Phys. Rev. A **105**, 022610 (2022).

[14] D. Cozzolino, B. Da Lio, D. Bacco, and L. K. Oxenløwe, Adv. Quantum Technol. **2**, 1900038 (2019).

[15] K. Wei, N. Tischler, S.-R. Zhao, Y.-H. Li, J. M. Arrazola, Y. Liu, W. Zhang, H. Li, L. You, Z. Wang, Y.-A. Chen, B. C. Sanders, Q. Zhang, G. J. Pryde, F. Xu, and J.-W. Pan, Phys. Rev. Lett. **122**, 120504 (2019).

[16] M. Erhard, R. Fickler, M. Krenn, and A. Zeilinger, Light Sci. Appl. **7**, 17146 (2018).

[17] P. J. Low, B. M. White, A. A. Cox, M. L. Day, and C. Senko, Phys. Rev. Research **2**, 033128 (2020).

[18] M. Neeley, M. Ansmann, R. C. Bialczak, M. Hofheinz, E. Lucero, A. D. O'Connell, D. Sank, H. Wang, J. Wenner, A. N. Cleland, M. R. Geller, and J. M. Martinis, Science **325**, 722 (2009).

[19] V. A. Soltamov, C. Kasper, A. V. Poshakinskiy, A. N. Anisimov, E. N. Mokhov, A. Sperlich, S. A. Tarasenko, P. G. Baranov, G. V. Astakhov, and V. Dyakonov, Nat. Commun. **10**, 1678 (2019).

[20] F. D. M. Haldane, Phys. Rev. Lett. **50**, 1153 (1983).

[21] F. D. M. Haldane, Bull. Am. Phys. Soc. **27**, 181 (1982).

[22] H. J. Schulz, Phys. Rev. B **34**, 6372 (1986).

[23] J. B. Parkinson, J. C. Bonner, G. Müller, M. P. Nightingale, and H. W. J. Blöte, J. Appl. Phys. **57**, 3319 (1985).

[24] O. F. de Alcantara Bonfim and T. Schneider, Phys. Rev. B **30**, 1629 (1984).

[25] I. Affleck, T. Kennedy, E. H. Lieb, and H. Tasaki, Phys. Rev. Lett. **59**, 799 (1987).

[26] I. Affleck, T. Kennedy, E. H. Lieb, and H. Tasaki, Commun. Math. Phys. **115**, 477 (1988).

[27] Y. Heng Su, S. Young Cho, B. Li, H.-L. Wang, and H.-Q. Zhou, J. Phys. Soc. Jpn. **81**, 074003 (2012).

[28] R. Alicki and M. Fannes, Phys. Rev. E **87**, 042123 (2013).

[29] F. Campaioli, F. A. Pollock, and S. Vinjanampathy, arXiv:1805.05507.

[30] K. V. Hovhannisyan, M. Perarnau-Llobet, M. Huber, and A. Acín, Phys. Rev. Lett. **111**, 240401 (2013).

[31] F. C. Binder, S. Vinjanampathy, K. Modi, and J. Goold, New J. Phys. **17**, 075015 (2015).

[32] F. Campaioli, F. A. Pollock, F. C. Binder, L. Céleri, J. Goold, S. Vinjanampathy, and K. Modi, Phys. Rev. Lett. **118**, 150601 (2017).

[33] D. Ferraro, M. Campisi, G. M. Andolina, V. Pellegrini, and M. Polini, Phys. Rev. Lett. **120**, 117702 (2018).

[34] T. P. Le, J. Levinsen, K. Modi, M. M. Parish, and F. A. Pollock, Phys. Rev. A **97**, 022106 (2018).

[35] G. M. Andolina, M. Keck, A. Mari, M. Campisi, V. Giovannetti, and M. Polini, Phys. Rev. Lett. **122**, 047702 (2019).

[36] D. Farina, G. M. Andolina, A. Mari, M. Polini, and V. Giovannetti, Phys. Rev. B **99**, 035421 (2019).

[37] A. C. Santos, B. Çakmak, S. Campbell, and N. T. Zinner, Phys. Rev. E **100**, 032107 (2019).

[38] F.-Q. Dou, Y.-J. Wang, and J.-A. Sun, Europhys. Lett. **131**, 43001 (2020).

[39] S. Ghosh, T. Chanda, and A. Sen(De), Phys. Rev. A **101**, 032115 (2020).

[40] S. Ghosh, T. Chanda, S. Mal, and A. Sen (De), Phys. Rev. A **104**, 032207 (2021).

[41] A. Crescente, M. Carrega, M. Sassetti, and D. Ferraro, Phys. Rev. B **102**, 245407 (2020).

[42] M. Carrega, A. Crescente, D. Ferraro, and M. Sassetti, New J. Phys. **22**, 083085 (2020).

[43] D. Rossini, G. M. Andolina, D. Rosa, M. Carrega, and M. Polini, Phys. Rev. Lett. **125**, 236402 (2020).

[44] G. M. Andolina, M. Keck, A. Mari, V. Giovannetti, and M. Polini, Phys. Rev. B **99**, 205437 (2019).

[45] D. Rossini, G. M. Andolina, and M. Polini, Phys. Rev. B **100**, 115142 (2019).

[46] D. Rosa, D. Rossini, G. M. Andolina, M. Polini, and M. Carrega, J. High Energy Phys. 11 (2020) 067.

[47] J. Q. Quach and W. J. Munro, Phys. Rev. Appl. **14**, 024092 (2020).

[48] A. S. T. Pires, Phys. Rev. B **53**, 235 (1996).

[49] M. Mercaldo, I. Rabuffo, L. De Cesare, and A. Caramico D'Auria, J. Magn. Magn. Mater. **403**, 68 (2016).

[50] C. K. Lai, J. Math. Phys. **15**, 1675 (1974).

[51] L. Takhtajan, Phys. Lett. A **87**, 479 (1982).

[52] B. Sutherland, Phys. Rev. B **12**, 3795 (1975).

[53] H. Babujian, Phys. Lett. A **90**, 479 (1982).

[54] G. Fáth and J. Sólyom, Phys. Rev. B **44**, 11836 (1991).

[55] G. Fáth and J. Sólyom, Phys. Rev. B **47**, 872 (1993).

[56] K. Buchta, G. Fáth, O. Legeza, and J. Sólyom, Phys. Rev. B **72**, 054433 (2005).

[57] R. Mao, Y.-W. Dai, S. Y. Cho, and H.-Q. Zhou, Phys. Rev. B **103**, 014446 (2021).

[58] Z.-X. Gong, M. F. Maghrebi, A. Hu, M. Foss-Feig, P. Richerme, C. Monroe, and A. V. Gorshkov, Phys. Rev. B **93**, 205115 (2016).

[59] F. T. Tabesh, F. H. Kamin, and S. Salimi, Phys. Rev. A **102**, 052223 (2020).

[60] A. Crescente, M. Carrega, M. Sassetti, and D. Ferraro, New J. Phys. **22**, 063057 (2020).

[61] https://titaschanda.github.io/QIClib.

Correction: The affiliation was presented incorrectly and has been fixed.